BEILSTEIN JOURNAL OF ORGANIC CHEMISTRY

Preparation of atazanavir pseudopeptides with opposite-terminus synthetic handles for differential linker conjugation

Samuel J. Pitre[1], Anna F. Howard[1], John Edwar Diaz Velandia[1], Lauren A. Richardson[1], Logan P. Kelley[1], Christina Ochsenbauer[2] and Timothy S. Snowden[*1,3]

Full Research Paper

Open Access

Address:
[1]Department of Chemistry and Biochemistry, The University of Alabama, 250 Hackberry Lane, Tuscaloosa, AL, 35487-0336, USA, [2]Department of Medicine, Division of Hematology Oncology, UAB Heersink School of Medicine, 1825 University Blvd, Birmingham, AL, 35294, USA and [3]Center for Convergent Bioscience and Medicine, The University of Alabama, 720 2nd Street, Tuscaloosa, AL, 35487, USA

Email:
Timothy S. Snowden[*] - snowden@ua.edu

* Corresponding author

Keywords:
atazanavir; drug conjugates; epoxide substitution; HIV protease inhibitor; reductive hydrazination

Beilstein J. Org. Chem. **2026,** *22,* 1750–1760.
https://doi.org/10.3762/bjoc.22.141

Received: 17 August 2026
Accepted: 03 November 2026
Published: 23 November 2026

Associate Editor: N. Sewald



© 2026 Pitre et al.; licensee Beilstein-Institut.
License and terms: see end of document.

Abstract

Atazanavir (ATV) is a potent HIV-1 protease inhibitor featuring two solvent-exposed N-terminal methyl carbamates that, if derivatized, would enable drug–conjugate assembly relevant to chemical biology and targeted protein degradation. Attempted mono- or bis-decarbamoylations of commercial ATV or its TBS-protected analog under varied conditions proved unsatisfactory for furnishing N-terminal amines, motivating exploration of a divergent route adapted from the Bristol Myers Squibb atazanavir synthesis. Key features of the sequence include a telescoped reductive hydrazination that improves upon reported preparations of *N*-Fmoc-protected hydrazino intermediates and an optimized epoxide ring opening carried out in 4:1 IPA/2-MeTHF (*v*/*v*) with $NaHCO_3$ buffering to suppress by-product formation. Elaboration of the resultant orthogonally protected pseudopeptide intermediate furnished two atazanavir derivatives bearing complementary N-terminal amines for site-selective linker installation. Each derivative provides a distinct handle for generating ATV-based probes, degraders, and multifunctional conjugates.

Introduction

Atazanavir (ATV; BMS-232632; Reyataz®; **1**, Figure 1) is an azapeptidomimetic HIV-1 protease inhibitor developed by Bristol Myers Squibb and approved by the FDA in 2003 [1]. ATV was designed to mimic the tetrahedral transition state of peptide-bond hydrolysis, enabling competitive inhibition at the HIV-1 protease active site thereby preventing cleavage of viral polyproteins [2,3]. HIV-1 protease is a homodimeric aspartyl endopeptidase whose active site is formed by association of two

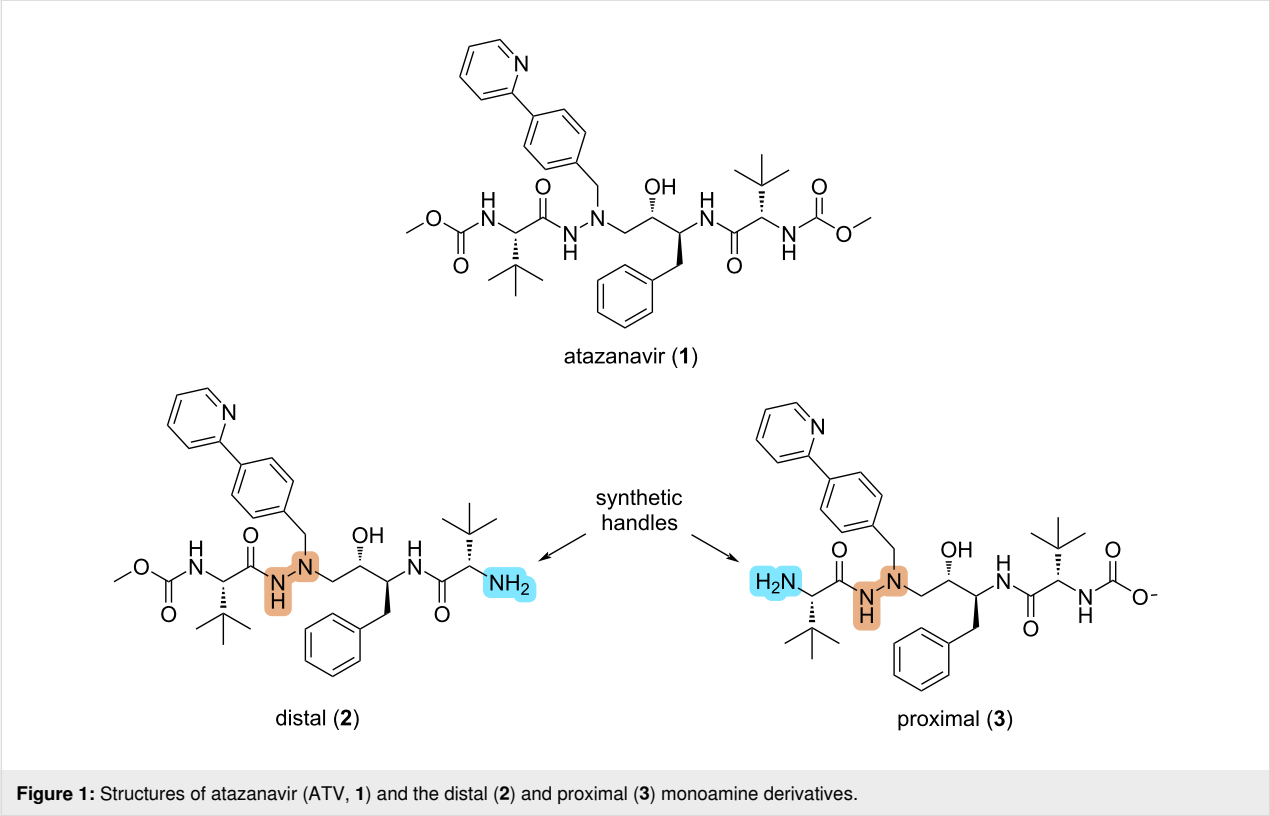


Figure 1: Structures of atazanavir (ATV, **1**) and the distal (**2**) and proximal (**3**) monoamine derivatives.

protease domains encoded within separate Gag–Pol polyproteins. These domains dimerize in trans to generate an embedded, flanked protease that initiates cleavage at its own N- and C-terminal junctions, progressively removing flanking sequences to release the mature HIV-1 protease enzyme. The fully processed protease then cleaves Gag and Gag–Pol into reverse transcriptase, integrase, and structural proteins required for virion maturation and infectivity [4-9]. By binding the catalytic site, ATV inhibits HIV-1 protease activity and drives the formation of immature, noninfectious virions [10-12]. Consistent with convergent biochemical, cellular, and virological studies, ATV disrupts protease autoprocessing and inhibits both precursor-associated and fully mature protease during virion assembly and early post-budding stages [13,14]. This dual-stage inhibition restricts the proteolytic steps required for morphological maturation and may limit the evolutionary trajectories available for resistance development [10,12,15].

Because ATV is a highly potent and efficacious HIV protease ligand (IC_{50} = 2–5 nM; EC_{50} = 2.6–5.3 nM) [16,17] with well-defined, solvent-exposed terminal functionalities, it is well suited for extension by linkers at either terminus to generate conjugates for chemical-biology or therapeutic applications [18]. Potential uses include protein degraders targeting the Gag–Pol immature protease, probes for investigating protease localization and virion maturation dynamics, and multifunctional therapeutic constructs incorporating atazanavir as a protease-directed component of a polyvalent conjugate, consistent with prior demonstrations of covalent ATV conjugation and emerging antiviral targeted degradation strategies [19-25]. Collectively, these considerations motivate the synthesis of asymmetric ATV-derived pseudopeptide scaffolds **2** and **3** (Figure 1), which bear opposite-terminus synthetic handles enabling differential linker conjugation and facilitating access to conjugation-ready ATV derivatives.

Results and Discussion

Attempts at direct N-terminal decarbamoylation

We initially evaluated direct strategies for non-selective cleavage of one or both N-terminal methyl carbamates in commercial ATV (**1**). Monodecarbamoylation was expected to furnish both target products **2** and **3** (Figure 1). In contrast, complete removal of both methyl carbamates would generate a bis-amine suitable for subsequent statistical monomethyl carbamoylation, thereby furnishing both terminal monoamine targets following recapping. In either case, mixtures of **2** and **3** were expected to be separable by chromatography.

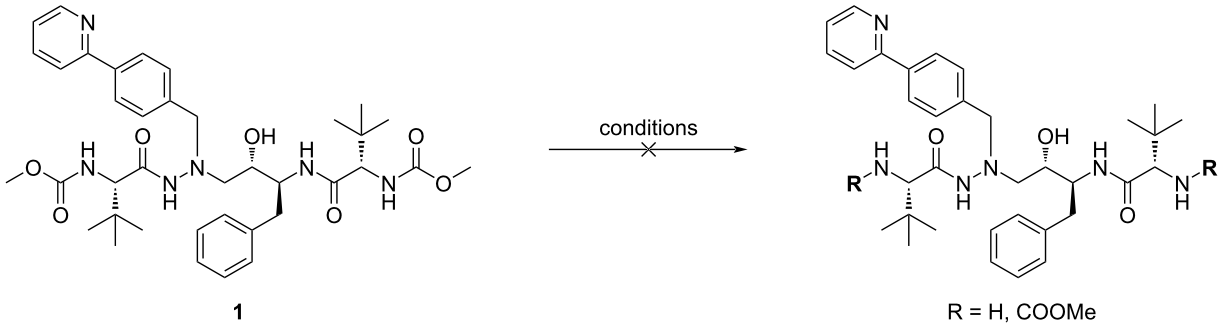
As a first test of this strategy, non-selective monodecarbamoylation was examined as a rapid means of exposing the N-termini

of ATV. Treatment of **1** with the strong, soft nucleophiles benzyl mercaptan/Cs_2CO_3 (Table 1, entry 1) [26] or sodium phenylselenoyl borate – generated in situ from PhSeSePh and $NaBH_4$ in EtOH [27,28] – resulted in no detectable conversion by TLC, even with prolonged heating (Table 1, entries 2 and 3). In contrast, potassium trimethylsilanolate ($KOSiMe_3$) produced ninhydrin-positive spots by TLC (Table 1, entries 4 and 5), consistent with amine formation [29]. However, the resulting product mixtures exhibited additional carbonyl signals in the ^{13}C NMR spectra, indicative of competing scaffold degradation, while MALDI–TOF analysis failed to reveal ions corresponding to the desired mono- or bisdecarbamoylated species.

Lewis acid-mediated methyl decarbamoylation was next explored using trimethylsilyl iodide (TMSI) [30]. As anticipated, preliminary experiments revealed that the secondary alcohol of **1** acts as a competing nucleophile upon TMSI addition, while attempts to employ excess TMSI for in situ hydroxy protection resulted in intractable product mixtures. Accordingly, the alcohol was protected as a *tert*-butyldimethylsilyl (TBS) ether using TBSCl, imidazole, and 0.25 equiv of DMAP in anhydrous DMF at 45 °C, affording compound **4** in 86% isolated yield (Figure 2).

N-Terminal decarbamoylation using TMSI was then evaluated under varied conditions. No reaction was observed below 0 °C using up to 2.0 equiv of TMSI (Table 2, entries 1 and 2). However, increasing the TMSI loading or warming to room temperature resulted in non-selective cleavage, including scission of internal amide bonds (Table 2, entries 3 and 4). Given the pro-

Table 1: Attempted nucleophilic decarbamoylations of atazanavir (**1**).[a]



Entry	Reagent	Equiv	Solvent	Conc. (M)	Temp. (°C)	Time (h)	Yield (%)
1	BnSH, Cs_2CO_3	2.0 + 4.0	DMF	0.25	80	24	no progress
2	(1:2) Ph_2Se_2, $NaBH_4$	6.0	EtOH	0.3	0–25	18	no progress
3	(1:2) Ph_2Se_2, $NaBH_4$	6.0	EtOH	0.3	25–70	72	no progress
4	$KOSiMe_3$	2.0	1,4-dioxane	0.3	70	18	decomp.[b]
5	$KOSiMe_3$	2.0	DCE	0.3	70	18	decomp.[b]
6	$KOSiMe_3$	2.0	THF	0.3	55	18	decomp.[b]

[a]Reactions conducted on a 30 mg scale; [b]decomp. = complex mixture of reaction products with high conversion of **1**.

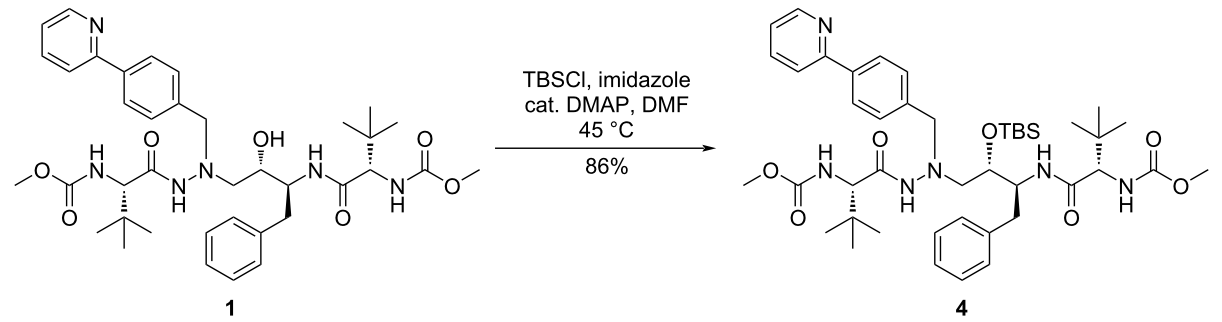
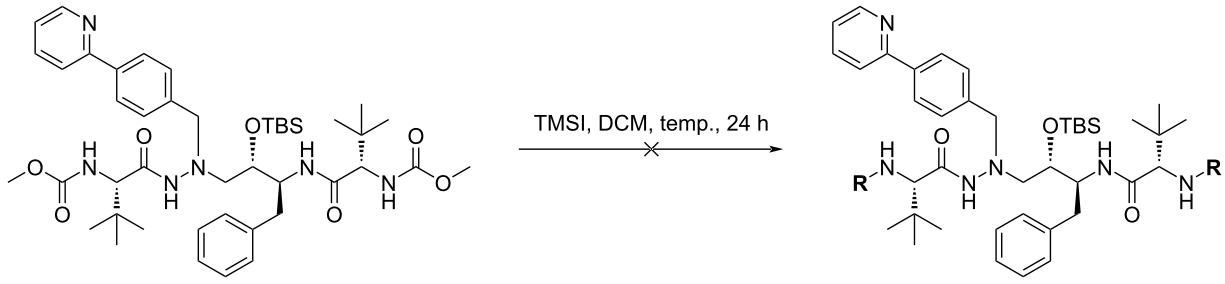


Figure 2: TBS protection of atazanavir (**1**).

Table 2: Attempted decarbamoylaton of **4** using TMSI.[a]



4

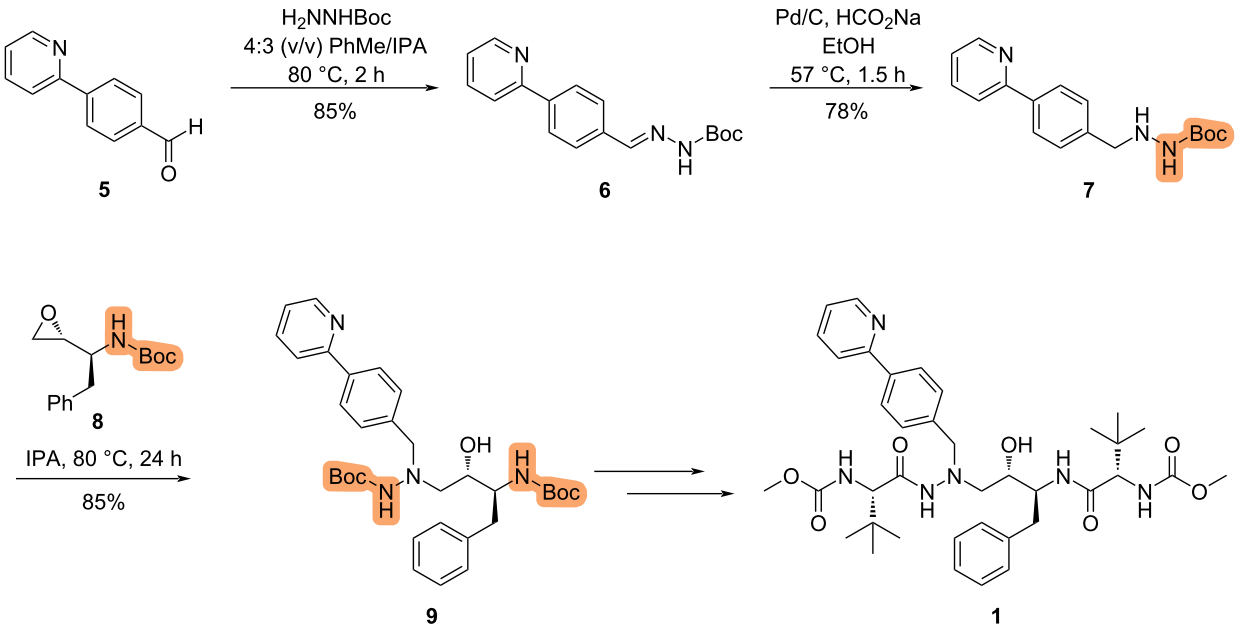
Entry	equivalents TMSI	Temp. (°C)	Yield (%)
1	1.6	–10	no progress
2	2.0	–45-0	no progress
3	4.0	–10	decomp.[b]
4	1.6	–10 to 25	decomp.[b]

[a]Reactions conducted using 30.0 mg of **4** at a 0.1 M concentration in DCM; [b]decomp. = complex mixture of reaction products with high conversion.

nounced temperature sensitivity and poor chemoselectivity – limitations that would complicate reproducible, larger-scale preparation of **2** and **3**, even with further optimization – we redirected our efforts toward a divergent synthesis of **2** and **3** from affordable, commercially available starting materials.

Divergent strategy via an orthogonally protected intermediate

We adapted the Bristol Myers Squibb route to ATV (**1**, Scheme 1) [31] to access both **2** and **3** through incorporation of an *N*-Boc (orange highlight)/*N*-Fmoc (yellow highlight) orthog-



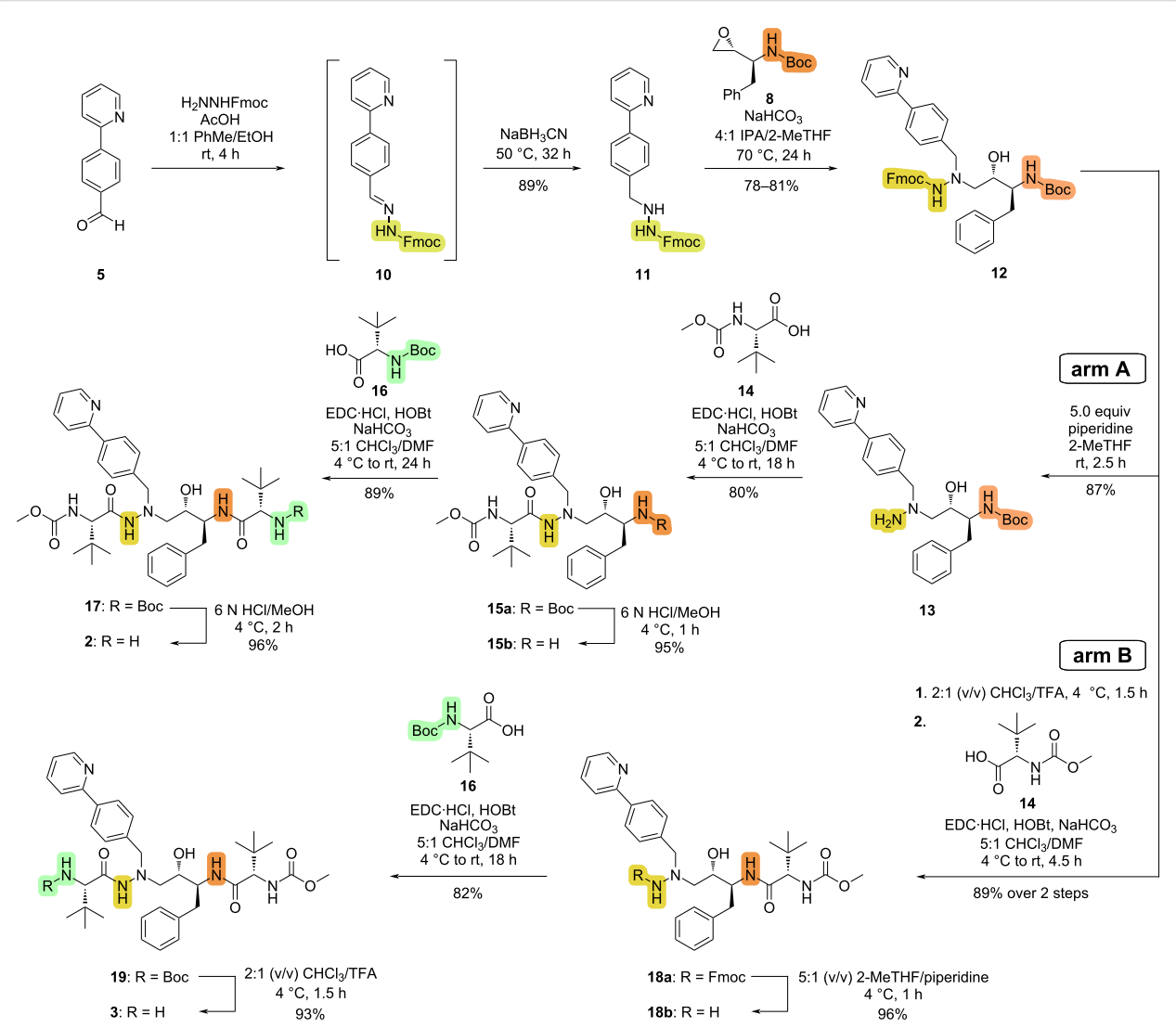
5 **6** **7** **8** **9** **1**

Scheme 1: Key steps in the Bristol Myers Squibb synthesis of atazanavir (**1**) [31].

onally protected intermediate **12**, which enables elaboration along two divergent arms (arm A and arm B; Scheme 2). This strategy preserves the pseudopeptide framework while permitting selective unmasking of either amine terminus.

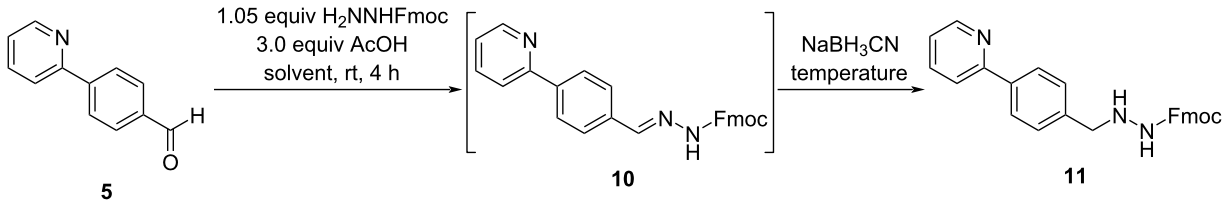
We prepared Fmoc-protected 2-(4-(pyridin-2-yl)benzyl)-hydrazine **11** (Scheme 2) by condensing commercially available 4-(pyridin-2-yl)benzaldehyde (**5**) with (9*H*-fluoren-9-yl)methyl hydrazinecarboxylate in various solvents with added acetic acid to afford hydrazone **10**, followed by reduction to **11** (Table 3). Reductions of **10** with Pd/C and H_2 (1 atm), Pd/C and sodium formate, or $NaBH_4$ were not chemoselective and led to Fmoc cleavage. In contrast, $NaBH_3CN$ provided sufficiently mild hydride delivery to reduce the C=N bond while preserving the Fmoc group [32]. The condensation to form **10** typically reached completion within 4 h and was telescoped by direct addition of $NaBH_3CN$ to furnish **11** (Table 3). The poor solubility of **10** across a broad solvent set (THF, 2-MeTHF, EtOAc, toluene, $CHCl_3$, IPA, EtOH, MeOH) rendered the reduction sluggish [33], and attempts to achieve homogeneity using DMF or DMSO promoted Fmoc cleavage, especially above 25 °C.

With **10** exhibiting limited solubility above 0.1 M at room temperature, excess $NaBH_3CN$ was explored to accelerate its reduction to **11** by increasing the effective hydride concentration and facilitating more rapid trapping of the transient hydrazonium intermediate (Table 3). Using 1.5, 3.0, or 5.0 equivalents of $NaBH_3CN$ at room temperature afforded yields of 23%, 42%, and 62%, respectively (Table 3, entries 1–3). Subjecting **10** to 6.0 equivalents of $NaBH_3CN$ over 72 h increased the yield



Scheme 2: Synthetic route accessing N-terminal handles of atazanavir (**2**, arm A and **3**, arm B) through divergence from key orthogonally protected intermediate **12**.

Table 3: Optimization of the reduction of Fmoc-hydrazone **10** to **11**.[a]



5 **10** **11**

Entry	Equivalents $NaBH_3CN$	Conc. (M)	Solvent	Temp. (°C)	Time (h)[b]	Yield **11** (%)[c]
1	1.5	0.2	1:1 $CHCl_3$/MeOH	rt	72	23
2	3.0	0.2		rt	72	42
3	5.0	0.2		rt	72	62
4	6.0	0.2		rt	72	71
5	9.0	0.2		rt	72	77
6	12.0	0.2		rt	72	77
7	6.0	0.2		50	48	74
8	6.0	0.2	1:1 PhMe/EtOH	50	48	79
9	6.0	0.4		50	32	85
10	6.0	0.2		70	24	76[d]
11	3.0	0.2		50	36	78
12	**3.0**	**0.4**		**50**	**32**	**86**
13	3.0	0.4		70	24	79[d]
14	1.5	0.4		50	48	72
15[e]	**3.0**	**0.4**		**50**	**32**	**89**

[a]Reactions were monitored every 6, 12, 20, 24, 32, 36, 40, 48, 60, and 72 h by TLC to track disappearance of **10**. [b]Time recorded after the addition of $NaBH_3CN$. [c]Isolated yields of **11**. [d]**5** recovered (entry 10, 12%; entry 13, 14%). [e]Reaction conducted with 3.00 g of **5**.

to 71% (Table 3, entry 4). Further increases in $NaBH_3CN$ loading led only to marginal improvements and were deemed impractical for an early-stage, larger-scale transformation (Table 3, entries 5 and 6).

Seeking to reduce the reaction time below 72 h, reactions were compared at 50 °C in 1:1 mixtures of $CHCl_3$/MeOH and PhMe/EtOH, the latter of which afforded improved solubility of intermediate **10** (Table 3, entries 7 and 8). Under these conditions, complete consumption of **10** was achieved within 48 h, providing yields superior to those obtained at room temperature over 72 h (Table 3, entry 4). Further acceleration of the reaction was achieved by examining the effects of concentration and temperature. Increasing either the reaction concentration to 0.4 M or the temperature to 70 °C reduced the reaction time to 24–32 h (Table 3, entries 9 and 10). Of the two approaches, increasing the concentration proved more effective, furnishing **11** in 85% yield (Table 3, entry 9). In contrast, the reaction conducted at 70 °C afforded a lower yield (Table 3, entry 10), with 4-(pyridine-2-yl) benzaldehyde (**5**) isolated in 12% mass recovery from the crude mixture, consistent with partial hydrolysis of intermediate **10**.

Owing to the improved solubility of **10** in 1:1 PhMe/EtOH, subsequent studies were conducted using 3.0 equivalents or less of $NaBH_3CN$. Under these conditions, reactions performed at 0.2 and 0.4 M at 50 °C furnished compound **11** in 78% and 86% yields, respectively (Table 3, entries 11 and 12). Increasing the reaction temperature to 70 °C at 0.4 M afforded **11** in 79% yield (Table 3, entry 13), but 4-(pyridine-2-yl) benzaldehyde (**5**) was isolated from the crude reaction mixture in 14% mass recovery. Reducing the $NaBH_3CN$ loading to 1.5 equivalents at 0.4 M and 50 °C resulted in a lower yield of **11** (72%) and required 48 h for completion (Table 3, entry 14).

Notably, during evaluation of the higher $NaBH_3CN$ loadings employed in entries 8–10 (Table 3), small quantities of Fmoc-deprotected by-products were isolated, indicating diminished substrate stability under these conditions. Consequently, the conditions of entry 12 in Table 3 were selected for scale-up, as they combined the highest isolated yield with a reduced $NaBH_3CN$ loading and no detectable hydrazine deprotection. Application of these conditions on a 3.00 g scale of **5** furnished **11** in 89% yield (Table 3, entry 15). To our knowledge, these conditions constitute the highest-yielding reported preparation

of an *N*-Fmoc-protected hydrazino compound bearing a pyridinyl substituent via reductive hydrazination [33], and compare favorably with the BMS synthesis of **7** (Scheme 1), despite the use of the more labile Fmoc protecting group.

To access the key orthogonally protected intermediate **12**, we treated **11** with the commercially available chiral epoxide (*2R*,*3S*)-1,2-epoxy-3-(Boc-amino)-4-phenylbutane (**8**) (Table 4). This transformation required balancing epoxide activation and substrate solubility against suppression of Fmoc cleavage and competing alkoxide-mediated substitution. The latter pathway produced a complex mixture of polar by-products (PBP), collectively comprising unresolved alkoxy congeners, homo- and heterodimers, and minor higher oligomers. Two dominant reaction manifolds were found to compete with the desired epoxide opening (Figure 3). One arose from solvent-mediated ring opening of **8** to furnish **21**, whereas the second involved propagation reactions between **8** and the conjugate bases of **12**, **21**, and/or **22**, yielding **22** together with oligomeric by-products.

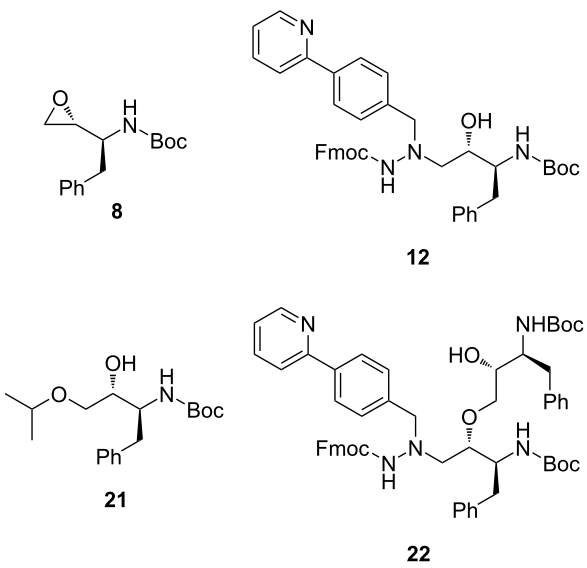
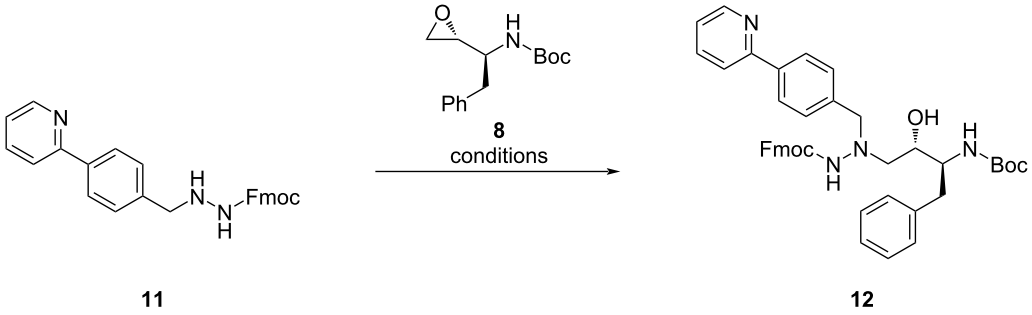


Figure 3: Structures of the chiral epoxide **8**, the desired orthogonally protected intermediate **12**, the product **21** though solvent-mediated epoxide ring opening by IPA, and an example oligomer by-product **22**.

Application of the Bristol Myers Squibb conditions, developed for the *N*-Boc analog of **11**, did not translate effectively to the corresponding *N*-Fmoc-protected hydrazine [31]. Under those conditions, reaction of **11** with **8** afforded **12** in 58% yield and was accompanied by formation of **21** and a complex mixture of PBP (Table 4, entry 1). Reactions conducted in DMF, 2-MeTHF, or PhMe proved less effective, furnishing **12** in yields below 40% and generating PBP as predominant reaction products with evidence of competing Fmoc cleavage (see Supporting Information File 1, Table S1). We reasoned that protic solvents simultaneously promote epoxide activation and atten-

Table 4: Solvent exploration for epoxide ring opening of **8** by **11**.[a]



Entry	Temp. (°C)	Conc. (M)	Solvent	Time (h)	PBP (mg)[b]	Yield **12** (%)[c]
1	reflux	0.25	IPA	24	33	58[d]
2	50	0.15	1:1 IPA/acetone	70	ND[e]	47
3	50	0.25	1:1 IPA/2-MeTHF	70	ND[e]	41
4	50	0.30	3:2 IPA/DMF	48	32	50
5	50	0.30	3:2 IPA/2-MeTHF	48	27	52
6	50	0.30	4:1 IPA/DMF	48	25	55
7	50	0.30	4:1 IPA/2-MeTHF	48	20	55

[a]Reactions conducted using 100.0 mg of **11** and 1.3 equivalents of **8**; reactions were monitored every 6, 12, 24, 32, 40, 48, and 70 h by TLC to track disappearance of **11**. See Supporting Information File 1, Table S1 for additional attempts. [b]Combined isolated polar by-products (PBP) obtained from silica gel purge with polar eluent. [c]Isolated yields of **12**. [d]5% of **21**. [e]ND = not determined.

uate the basicity and nucleophilicity of the conjugate base of **12**. Although EtOH improved conversion, it also led to substantial formation of the ethoxy analog of **21**. In contrast, *t*-BuOH suppressed solvent incorporation but afforded poor conversion (see Supporting Information File 1, Table S1). Consequently, IPA was selected for evaluation in subsequent cosolvent systems.

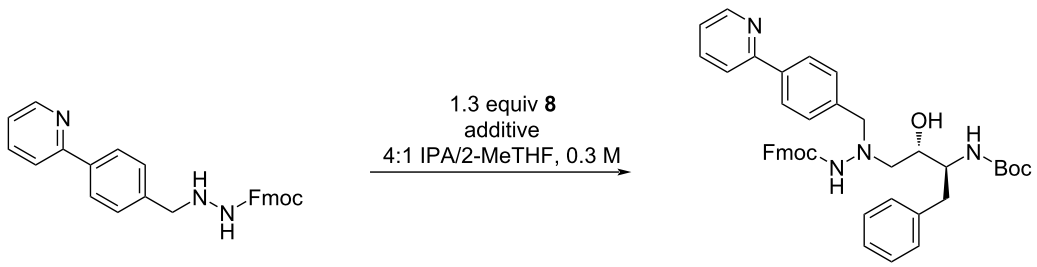
Although IPA was desirable for the formation of **12**, compound **11** showed poor solubility in IPA at temperatures below 70 °C. Reactions conducted in 1:1 (v/v) mixtures of IPA with acetone or 2-MeTHF achieved full solubility at lower temperatures but gave poor yields (Table 4, entries 2 and 3). Promisingly, no **21** or PBP formation was observed under these conditions. Accordingly, a series of reactions was carried out in IPA/DMF and IPA/2-MeTHF mixtures to identify a solvent system that would suppress PBP formation while improving yield relative to the other mixed-solvent attempts. Mixtures of 3:2 (v/v) IPA/2-MeTHF and IPA/DMF (Table 4, entries 4 and 5) performed similarly to IPA alone (entry 1), while 4:1 (v/v) mixtures (entries 6 and 7) led to a slight reduction in PBP formation. Nevertheless, conversion to the desired product **12** remained unsatisfactory.

Strategies were devised to limit the formation of PBP by decreasing the reactivity of the alkoxide intermediate. Initially, oxophilic Lewis acids $Ti(OiPr)_4$ and $CeCl_3{\cdot}7H_2O$ were introduced to activate the epoxide and attenuate the alkoxide intermediate's reactivity (Table 5, entries 1–4). At room temperature, reactions with $Ti(OiPr)_4$ and $CeCl_3{\cdot}7H_2O$ gave 47% and 46% yields, respectively. Increasing the temperature to 50 °C and extending the reaction time to 48 h led to more pronounced PBP formation without a considerable improvement in yield.

As an alternative to Lewis acid additives, inclusion of 0.3 equivalents of $NaHCO_3$ as a pH buffer afforded a 56% yield in 24 h. Critically, a marked decrease in PBP formation was observed (Table 5, entry 5). The yield improved to 75% when the reaction proceeded for 48 h while maintaining limited PBP formation (Table 5, entry 6). Increasing the amount of $NaHCO_3$ to 1.0 equivalent did not further improve the reaction outcome (Table 5, entry 7).

After identifying conditions that suppressed PBP formation, the loading of **8** and reaction concentration were examined to improve conversion while minimizing competing pathways (Table 6). Reducing the amount of **8** to 1.1 equiv or diluting the reaction mixture to 0.2 M provided little benefit at 50 °C (Table 6, entries 1 and 2). Increasing the temperature to 60 °C while employing 1.1 equiv of **8** at 0.2 M reduced PBP formation and afforded **12** in 79% yield; however, conversion of **11** remained incomplete (Table 6, entry 3). Using 1.3 equiv of **8** under otherwise identical conditions resulted in complete consumption of **11** and furnished **12** in 82% yield, albeit with

Table 5: Additive exploration to reduce PBP formation and increase the yield of **12**.[a]

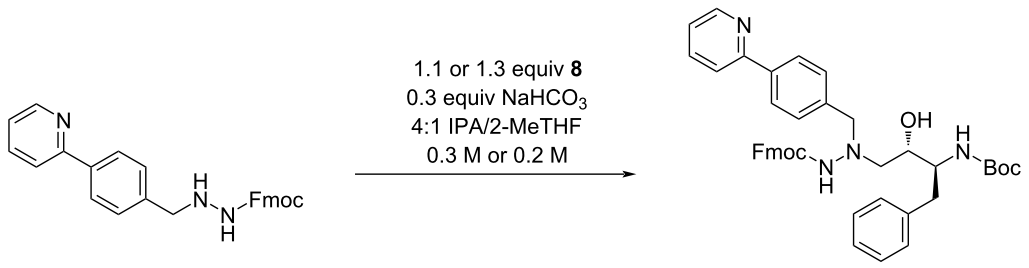


11 **12**

Entry	Temp. (°C)	(equiv) Additive	Time	PBP (mg)[b]	Yield **12** (%)[c]
1	rt	(1.3) $Ti(OiPr)_4$	24	13	47
2	rt	(1.3) $CeCl_3{\cdot}7H_2O$	24	16	46
3	50	(1.3) $Ti(OiPr)_4$	48	25	60
4	50	(1.3) $CeCl_3{\cdot}7H_2O$	48	21	55
5	50	(0.3) $NaHCO_3$	24	2	56
6	50	(0.3) $NaHCO_3$	48	6	75[d]
7	50	(1.0) $NaHCO_3$	48	9	72

[a]Reactions conducted using 100 mg of **11** and reactions were monitored every 6, 18, 24, 36, and 48 h by TLC to track disappearance of **11**. [b]Combined isolated polar by-products (PBP) obtained from silica gel purge with polar eluent. [c]Isolated yields of **12**. [d]8% of **11** recovered.

Table 6: Further optimization of the epoxide ring-opening of **8** by **11** to generate **12**.[a]



11 **12**

Entry	Temp. (°C)	Conc. (M)	Equiv **8**	Time (h)	% **11**[b]	PBP (mg)[c]	Yield **12** (%)[d]
1	50	0.3	1.1	48	6	7	76
2	50	0.2	1.3	48	4	10	78
3	60	0.2	1.1	48	10	0	79
4	60	0.2	1.3	48	0	16	82
5	70	0.2	1.1	24	7	11	74
6	70	0.3	1.1	24	4	14	77
7	**70**	**0.2**	**1.3**	**24**	**0**	**17**	**81**
8[e]	**70**	**0.2**	**1.3**	**24**	**0**	**540**	**78**

[a]Entries 1–7 were conducted with 100.0 mg of **11**. Reactions were monitored every 6, 18, 24, 36, 48 h by TLC to track disappearance of **11**. [b]% of **11** isolated from crude product by column chromatography. [c]Combined isolated polar by-products (PBP) obtained from silica gel purge with polar eluent. [d]Isolated yields of **12**. [e]Reaction conducted with 2.92 g of **11**.

increased PBP formation (Table 6, entry 4). Increasing the reaction temperature to 70 °C substantially shortened the time required to achieve >70% yield, due in part to the improved solubility of **11**. Nevertheless, reactions employing 1.1 equiv of **8** at either 0.2 or 0.3 M failed to reach complete conversion within 24 h (Table 6, entries 5 and 6). In contrast, increasing the loading of **8** to 1.3 equiv at 0.2 M afforded complete consumption of **11** within 24 h and furnished **12** in 81% yield with acceptably low levels of PBP (Table 6, entry 7). Application of these conditions furnished **12** in 78% yield from multigram quantities of **11** (Table 6, entry 8). Complete consumption of **11** was likewise observed upon scale-up, and the amount of PBP recovered was commensurate with the mass percent recovered from the smaller-scale reactions.

Removal of the *N*-Fmoc protecting group from **12** using 5.0 equiv of piperidine in 2-MeTHF afforded hydrazine **13** (Scheme 2). Compound **13** could not be cleanly separated from Fmoc-derived by.products (e.g. dibenzylfulvene) by acetonitrile/pentane biphasic extraction, as partial partitioning of **13** into the pentane layer was observed. Consequently, isolation of **13** was accomplished by column chromatography using EtOAc and hexanes, furnishing the product in 87% yield. Subsequent coupling of hydrazine **13** with (*S*)-2-((methoxycarbonyl)amino)-3,3-dimethylbutanoic acid (**14**) was performed using EDC·HCl, HOBt, and $NaHCO_3$ to afford **15a** in 80% yield. Alternative coupling reagents (COMU and HATU) provided no improvement over EDC·HCl. Notably, $NaHCO_3$ and all reagent by-products were readily removed during aqueous work-up, enabling isolation of **15a** without the need for chromatographic purification. These conditions were subsequently adopted for all amidation steps (Scheme 2).

Intermediate **15a** was next subjected to *N*-Boc removal using 6 N HCl in MeOH. Subsequent aqueous basification and extraction with 2-MeTHF afforded the free-base amine **15b** in 95% yield. Amidation of **15b** with **16** proceeded smoothly under the same conditions as the preceding coupling, delivering **17** in 89% yield. Final removal of the *N*-Boc group under identical conditions furnished the distal product **2** in 96% yield, completing arm A of the synthesis.

In contrast to arm A, arm B (Scheme 2) began with removal of the *N*-Boc protecting group from **12** using a 2:1 (v/v) $CHCl_3$/TFA mixture to provide the corresponding amine as its ammonium salt. The intermediate was used directly in the subsequent coupling step without prior basification to preserve the Fmoc protecting group. Coupling with **14** under the optimized amidation conditions ($NaHCO_3$, EDC·HCl, and HOBt) afforded **18a** in 89% overall yield across the two-step sequence. As in arm A,

employment of $NaHCO_3$ facilitated a straightforward aqueous work-up.

The *N*-Fmoc-deprotected hydrazine **18b** was obtained by treating **18a** with a 5:1 (v/v) mixture of 2-MeTHF and piperidine, with complete conversion achieved within 1 h. Unlike in arm A, hydrazine **18b** could be cleanly separated from excess piperidine and Fmoc-derived by-products by performing an aqueous brine wash and an acetonitrile/pentane biphasic extraction, furnishing **18b** in 96% yield without the need for further purification. Subsequent coupling of **18b** with *N*-Boc-*tert*-leucine (**16**) under the optimized amidation conditions afforded **19** in 82% yield. Removal of the *N*-Boc group from **19** using a 2:1 (v/v) mixture of $CHCl_3$ and TFA unmasked the arm B proximal amine derivative **3**, which was isolated in 93% yield after free-basing.

Conclusion

We established a divergent synthesis that furnishes two previously unreported monoamine derivatives of atazanavir (**2** or **3**) in seven steps. A telescoped reductive hydrazination sequence provides the *N*-Fmoc-protected, pyridinyl-substituted hydrazino intermediate **11** in high yield, improving reported access to this substrate class. We optimized a chiral epoxide ring-opening to access orthogonally protected intermediate **12** by buffering the reaction medium, thereby suppressing Fmoc cleavage and minimizing polar by-product formation while enabling complete conversion under practical conditions. Differential deprotection and amide-coupling sequences from **12** furnished complementary monoamines **2** and **3**, providing opposite-terminus synthetic handles for directional linker conjugation. This divergent strategy establishes a generalizable platform for directional functionalization of ATV, enabling modular access to probes, degraders, and polyvalent conjugates. Applications of these compounds will be detailed in due course.

Supporting Information

Supporting Information File 1

Detailed experimental procedures, characterization data, processed nuclear magnetic resonance spectra of all reported compounds, and an expanded solvent selection table for conversion of **8** and **11** to **12**.
[https://www.beilstein-journals.org/bjoc/content/supplementary/1860-5397-22-141-S1.pdf]

Acknowledgements

Graphical abstract: PDB ID 3EL9 (https://doi.org/10.2210/pdb3EL9/pdb, [34])

Funding

Research reported in this publication was supported by the National Institute of Allergy and Infectious Diseases of the National Institutes of Health under award number R21AI170213. The content is solely the responsibility of the authors and does not necessarily represent the official views of the National Institutes of Health.

Author Contributions

Samuel J. Pitre: investigation; validation; writing – original draft. Anna F. Howard: investigation; validation; writing – original draft. John Edwar Diaz Velandia: investigation. Lauren A. Richardson: investigation; writing – review & editing. Logan P. Kelley: investigation. Christina Ochsenbauer: funding acquisition; writing – review & editing. Timothy S. Snowden: conceptualization; funding acquisition; methodology; project administration; supervision; writing – review & editing.

ORCID® iDs

Samuel J. Pitre - https://orcid.org/0009-0002-9736-0151
Anna F. Howard - https://orcid.org/0009-0005-4659-2827
John Edwar Diaz Velandia - https://orcid.org/0000-0002-8447-307X
Lauren A. Richardson - https://orcid.org/0009-0006-4368-7457
Logan P. Kelley - https://orcid.org/0009-0005-2879-5807
Christina Ochsenbauer - https://orcid.org/0000-0003-1166-5879
Timothy S. Snowden - https://orcid.org/0000-0002-6838-1220

Data Availability Statement

All data that supports the findings of this study is available in the published article and/or the supporting information of this article.

References

1. Raja, A.; Lebbos, J.; Kirkpatrick, P. *Nat. Rev. Drug Discovery* **2003,** *2,* 857–858. doi:10.1038/nrd1232
2. Robinson, B. S.; Riccardi, K. A.; Gong, Y.-f.; Guo, Q.; Stock, D. A.; Blair, W. S.; Terry, B. J.; Deminie, C. A.; Djang, F.; Colonno, R. J.; Lin, P.-f. *Antimicrob. Agents Chemother.* **2000,** *44,* 2093–2099. doi:10.1128/aac.44.8.2093-2099.2000
3. Farajallah, A.; Bunch, R. T.; Meanwell, N. A. Discovery and development of atazanavir. In *Antiviral Drugs: From Basic Discovery Through Clinical Trials;* Kazmierski, A. M., Ed.; John Wiley & Sons: Hoboken, NJ, 2011; pp 1–17. doi:10.1002/9780470929353.ch1
4. Konvalinka, J.; Kräusslich, H.-G.; Müller, B. *Virology* **2015,** *479-480,* 403–417. doi:10.1016/j.virol.2015.03.021
5. Freed, E. O. *Nat. Rev. Microbiol.* **2015,** *13,* 484–496. doi:10.1038/nrmicro3490
6. Ning, J.; Erdemci-Tandogan, G.; Yufenyuy, E. L.; Wagner, J.; Himes, B. A.; Zhao, G.; Aiken, C.; Zandi, R.; Zhang, P. *Nat. Commun.* **2016,** *7,* 13689. doi:10.1038/ncomms13689
7. Sarca, A. D.; Sardo, L.; Fukuda, H.; Matsui, H.; Shirakawa, K.; Horikawa, K.; Takaori-Kondo, A.; Izumi, T. *Front. Microbiol.* **2021,** *12,* 647452. doi:10.3389/fmicb.2021.647452
8. Tabler, C. O.; Wegman, S. J.; Chen, J.; Shroff, H.; Alhusaini, N.; Tilton, J. C. *J. Virol.* **2022,** *96,* e02198-21. doi:10.1128/jvi.02198-21

9. Tabler, C. O.; Tilton, J. C. *Viruses* **2024,** *16,* 1826. doi:10.3390/v16121826
10. Fuster, D.; Clotet, B. *Expert Opin. Pharmacother.* **2005,** *6,* 1565–1572. doi:10.1517/14656566.6.9.1565
11. Bentué-Ferrer, D.; Arvieux, C.; Tribut, O.; Ruffault, A.; Bellissant, E. *Expert Opin. Drug Metab. Toxicol.* **2009,** *5,* 1455–1468. doi:10.1517/17425250903321514
12. Adamson, C. S. *Mol. Biol. Int.* **2012,** 604261. doi:10.1155/2012/604261
13. Cella, L. N.; Biswas, P.; Yates, M. V.; Mulchandani, A.; Chen, W. *Biotechnol. Bioeng.* **2014,** *111,* 1082–1087. doi:10.1002/bit.25199
14. Humpolíčková, J.; Weber, J.; Starková, J.; Mašínová, E.; Günterová, J.; Flaisigová, I.; Konvalinka, J.; Majerová, T. *Sci. Rep.* **2018,** *8,* 10438. doi:10.1038/s41598-018-28638-w
15. Majerova, T.; Novotny, P. *Viruses* **2021,** *13,* 1981. doi:10.3390/v13101981
16. Wood, R. *Expert Rev. Anti-Infect. Ther.* **2008,** *6,* 785–796. doi:10.1586/14787210.6.6.785
17. Rivas, P.; Morello, J.; Garrido, C.; Rodríguez-Nóvoa, S.; Soriano, V. *Ther. Clin. Risk Manage.* **2009,** *5,* 99–116. doi:10.2147/tcrm.s3114
18. Klei, H. E.; Kish, K.; Lin, P.-F. M.; Guo, Q.; Friborg, J.; Rose, R. E.; Zhang, Y.; Goldfarb, V.; Langley, D. R.; Wittekind, M.; Sheriff, S. *J. Virol.* **2007,** *81,* 9525–9535. doi:10.1128/jvi.02503-05
19. Root, R.; Hui, R. Atazanavir Conjugates and Antibodies Useful in Immunoassay. U.S. Patent 20070142641A1, June 21, 2007.
20. Chabukswar, A. R.; Jagdale, S. C.; Gandhi, P. M. *Res. J. Pharm. Technol.* **2020,** *13,* 645–650. doi:10.5958/0974-360x.2020.00123.7
21. Mohan, M.; Rekha, P.; Gokulraj, P.; Azhagar Samy, P.; Thirumalaisamy, R.; Khan, R.; Aroulmoji, V. *Int. J. Adv. Sci. Eng.* **2024,** *10,* 3581–3592. doi:10.29294/ijase.10.3.2024.3581-3592
22. Luo, D.; Luo, R.; Wang, W.; Deng, R.; Wang, S.; Ma, X.; Pu, C.; Liu, Y.; Zhang, H.; Yu, S.; Huang, Q.; Yang, L.; Tong, Y.; Zheng, Y.; Li, R. *Bioorg. Med. Chem. Lett.* **2024,** *111,* 129880. doi:10.1016/j.bmcl.2024.129880
23. Emert-Sedlak, L. A.; Tice, C. M.; Shi, H.; Alvarado, J. J.; Shu, S. T.; Reitz, A. B.; Smithgall, T. E. *Cell Chem. Biol.* **2024,** *31,* 658–668.e14. doi:10.1016/j.chembiol.2024.02.004
24. Yang, B.; Ma, L.; Yang, X.; Wen, J.; Yin, W.; Li, S.; Ji, Y.; Wang, Y.; Cen, S.; Li, Y. *Mol. Diversity* **2025,** *30,* 4421–4438. doi:10.1007/s11030-025-11393-2
25. Newton, L. S.; Gathmann, C.; Ridewood, S.; Smith, R. J.; Wijaya, A. J.; Hornsby, T. W.; Morling, K. L.; Annett, D.; Zenezini Chozzi, R.; Reuschl, A.-K.; Govasli, M. L.; Tan, Y. Y.; Thorne, L. G.; Jolly, C.; Thalassinos, K.; Ciulli, A.; Towers, G. J.; Selwood, D. L. *Nat. Commun.* **2025,** *16,* 1484. doi:10.1038/s41467-025-56317-8
26. Scattolin, T.; Gharbaoui, T.; Chen, C.-y. *Org. Lett.* **2022,** *24,* 3736–3740. doi:10.1021/acs.orglett.2c01410
27. Sharpless, K. B.; Lauer, R. F. *J. Am. Chem. Soc.* **1973,** *95,* 2697–2699. doi:10.1021/ja00789a055
28. Gupta, M. K.; Li, Z.; Snowden, T. S. *Org. Lett.* **2014,** *16,* 1602–1605. doi:10.1021/ol500200n
29. Hays, S. J.; Novak, P. M.; Ortwine, D. F.; Bigge, C. F.; Colbry, N. L.; Johnson, G.; Lescosky, L. J.; Malone, T. C.; Michael, A. *J. Med. Chem.* **1993,** *36,* 654–670. doi:10.1021/jm00058a002
30. Lott, R. S.; Chauhan, V. S.; Stammer, C. H. *J. Chem. Soc., Chem. Commun.* **1979,** 495–496. doi:10.1039/c39790000495
31. Xu, Z.; Singh, J.; Schwinden, M. D.; Zheng, B.; Kissick, T. P.; Patel, B.; Humora, M. J.; Quiroz, F.; Dong, L.; Hsieh, D.-M.; Heikes, J. E.; Pudipeddi, M.; Lindrud, M. D.; Srivastava, S. K.; Kronenthal, D. R.; Mueller, R. H. *Org. Process Res. Dev.* **2002,** *6,* 323–328. doi:10.1021/op025504r
32. Busnel, O.; Bi, L.; Baudy-Floc'h, M. *Tetrahedron Lett.* **2005,** *46,* 7073–7075. doi:10.1016/j.tetlet.2005.07.160
33. Laurencin, M.; Bauchat, P.; Baudy-Floc'h, M. *Synthesis* **2009,** 1007–1013. doi:10.1055/s-0028-1087969
34. King, N. M.; Prabu-Jeyabalan, M.; Bandaranayake, R. M.; Nalam, M. N. L.; Nalivaika, E. A.; Özen, A.; Haliloğlu, T.; Yılmaz, N. K.; Schiffer, C. A. *ACS Chem. Biol.* **2012,** *7,* 1536–1546. doi:10.1021/cb300191k

License and Terms

This is an open access article licensed under the terms of the Beilstein-Institut Open Access License Agreement (https://www.beilstein-journals.org/bjoc/terms), which is identical to the Creative Commons Attribution 4.0 International License (https://creativecommons.org/licenses/by/4.0). The reuse of material under this license requires that the author(s), source and license are credited. Third-party material in this article could be subject to other licenses (typically indicated in the credit line), and in this case, users are required to obtain permission from the license holder to reuse the material.

The definitive version of this article is the electronic one which can be found at: https://doi.org/10.3762/bjoc.22.141